

ENVIRONMENTAL RESEARCH  
LETTERS

## LETTER

## Elevation-dependent warming in the Eastern Siberian Arctic

James R Miller<sup>1</sup> , John E Fuller<sup>1</sup>, Michael J Puma<sup>2,3</sup> and Joseph M Finnegan<sup>1</sup> RECEIVED  
19 October 2020REVISED  
4 January 2021ACCEPTED FOR PUBLICATION  
13 January 2021PUBLISHED  
10 February 2021<sup>1</sup> Department of Marine and Coastal Sciences, Rutgers University, New Brunswick, NJ, United States of America<sup>2</sup> Center for Climate Systems Research, Columbia University, New York, NY, United States of America<sup>3</sup> NASA Goddard Institute for Space Studies, New York, NY, United States of AmericaE-mail: [mjp38@columbia.edu](mailto:mjp38@columbia.edu)**Keywords:** elevation-dependent warming, Arctic warming, Arctic amplification, temperature inversions

Original content from this work may be used under the terms of the [Creative Commons Attribution 4.0 licence](https://creativecommons.org/licenses/by/4.0/).

Any further distribution of this work must maintain attribution to the author(s) and the title of the work, journal citation and DOI.

**Abstract**

There is evidence for elevation-dependent warming (EDW) in many mountainous regions, including the Alps, Rockies, and Tibetan Plateau, all of which are in mid latitudes. Most studies finding evidence of EDW indicate that both recent decadal and future projected warming rates are greater at higher elevations. In this study, we examine the roles of Arctic amplification and elevation on future warming rates in winter and summer in eastern Siberia (50–70° N; 80–180° E). This region includes four major river basins that flow into the Arctic Ocean (the Yenisei, Lena, Indigirka, and Kolyma) and intersects with mountain ranges in northern Mongolia and eastern Siberia. We analyze projected 21st century temperature projections using a six-member ensemble of the National Center for Atmospheric Research (NCAR) Community Climate System Model (CCSM4) with a radiative forcing of 8.5 W m<sup>-2</sup>. Projected warming rates in winter for the 21st century are dominated by Arctic amplification, which leads to significantly larger warming rates at higher latitudes, with latitudinal gradients of about 0.16 °C degree<sup>-1</sup> latitude. In summer, the latitudinal gradient is near zero (0.02 °C degree<sup>-1</sup> of latitude). Within specific latitude bands, we also find EDW. However, unlike most mid-latitude locations where warming rates are greater at higher elevations, we find that future warming rates are smaller at higher elevations for this high-latitude region, particularly during winter, with statistically significant rates varying between -0.70 °C km<sup>-1</sup> and -2.46 °C km<sup>-1</sup> for different 5° latitude bands. The decrease in warming rates with elevation in winter at the highest latitudes is primarily attributed to strong inversions and changes in the lapse rate as free-air temperatures warm at slower rates than surface temperatures. In summer, the elevation dependence is much weaker than in winter but still statistically significant and negative in all but the most northern latitude band with values ranging between -0.10 °C km<sup>-1</sup> and -0.56 °C km<sup>-1</sup>.

**1. Introduction**

Temperatures in the Arctic have been increasing at an enhanced rate relative to the global average, which is referred to as Arctic amplification (Serreze *et al* 2009, Screen and Simmonds 2010). In fact, Arctic near-surface air temperatures have risen almost twice as much as the global average during recent decades (Symon *et al* 2005, Serreze and Francis 2006, Solomon *et al* 2007). High-latitude river basins are a major component of the global hydrologic cycle, because they provide return paths for water to the ocean from latitudes where precipitation is typically heavy. Most of this return flow enters the Arctic Ocean, where it affects the stability of the water column, sea ice

formation, and ocean circulation—both within the Arctic and in the North Atlantic—through freshwater export.

High-latitude river systems generally have their headwaters in high-elevation regions. Several model studies have found that projected future increases in river flow are greatest at high northern latitudes, a result that is consistent with more recent studies (e.g. Miller and Russell 1992, Manabe *et al* 2004, Milly *et al* 2005, Rawlins *et al* 2010). Among questions not yet resolved are how the interactions among temperature, precipitation, and runoff will change in these river basins as the climate warms this century. It is also unknown how these interactions and projected changes are affected by Arctic amplification

and elevation. Importantly, Arctic amplification is not seasonally uniform; winter warming dominates the annual trend. Water vapor and cloud feedbacks are responsible for some of this winter enhancement (Miller *et al* 2007, Ghatak and Miller 2013).

There is a range of elevations in high northern latitudes, and based on studies primarily at lower latitudes, warming rates are often elevation dependent (Beniston *et al* 1997, Diaz and Bradley 1997). This result is based on observations during the last several decades as well as model projections for later this century, many of which indicate that temperature has been changing more rapidly at higher elevations than in the surrounding lowlands (Fyfe and Flato 1999, Bradley *et al* 2004, Ohmura 2012, Rangwala and Miller 2012, Scherrer *et al* 2012, Pepin *et al* 2015, Sharma and Déry 2016). There has been much less research on elevation-dependent warming (EDW) in mountains at high latitudes, partly because they are in sparsely populated or data sparse regions and because mountain systems there are not as high as some of the mid-latitude mountain systems more commonly studied. Although Wang *et al* (2016) used a global set of observations to sort out the roles of Arctic amplification and elevation on EDW, their data were sparse at the highest latitudes. Changes there, however, are important in terms of their interplay with the Arctic climate system, particularly the Arctic Ocean. As an example of hydrologic changes there, Rawlins *et al* (2010) examined hydrology in northern Eurasia and found that Arctic freshwater content is increasing in response to increases in precipitation (P), evapotranspiration (ET), and runoff. They also found that the changes in P–ET are different between summer and winter.

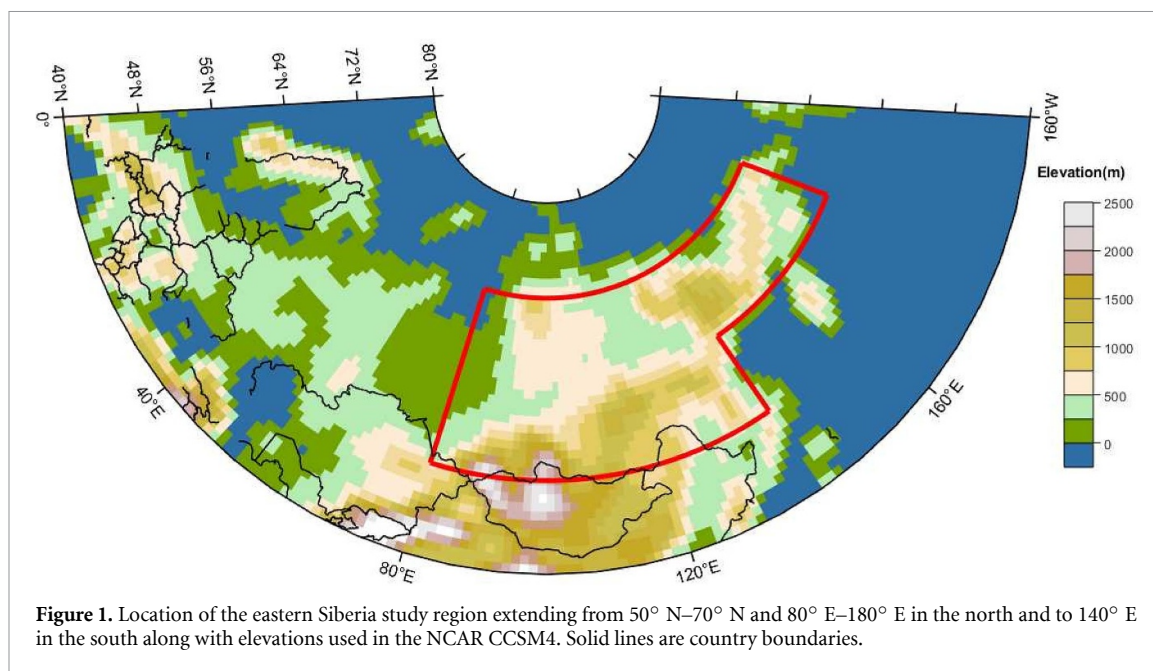
There are potential impacts of Arctic amplification that extend beyond the Arctic. Ghatak *et al* (2012) ran a suite of climate model experiments to isolate the role of Arctic Ocean surface conditions on Siberian snow cover and found that they affect Siberian snow depth, precipitation and air temperature. Francis and Vavrus (2012, 2015) examined how declining sea ice can affect mid-latitude weather. Temperature changes will affect the annual ratio of snowfall to rainfall as well as the timing of the snow accumulation and melt seasons, all of which will affect local surface and groundwater runoff and river flow. The freshwater fluxes from these river systems are important for ocean processes in the Arctic and in the North Atlantic (Sévellec *et al* 2017). Potential impacts of climate change on some of these high-latitude river basins has been examined (Gelfan *et al* 2017, Krysanova and Hattermann 2017). Furthermore, the continual decrease in Arctic summer sea ice extent has implications for the nearby terrestrial land mass, and although still controversial, may also have significant impacts on the Northern Hemisphere mid latitudes (Francis and Vavrus 2012, Cohen *et al* 2013).

In this paper, we examine projected 21st century trends in surface air temperature for summer and winter in an eastern Siberian region that includes four major river basins, the Yenisei, Lena, Indigirka, and Kolyma. The focus is on the role of Arctic amplification on the latitudinal variability of these temperature trends. Furthermore, we investigate whether projected temperature trends depend on elevation, and if so, whether that too is related to Arctic amplification. The National Center for Atmospheric Research (NCAR) Community Climate System Model (CCSM4) climate model is the primary model we use, but to investigate whether our results are robust or model dependent, we compare the results with projections from four other climate models.

## 2. Methodology and models

The primary climate model output used in this analysis is from the NCAR CCSM4, a general circulation climate model that is part of the Coupled Model Intercomparison Project's fifth phase (CMIP5), with atmospheric, land, and ocean resolutions of about  $1^\circ$  (Gent *et al* 2011). This model is used because it is well documented in the literature and has higher resolution than many of the other CMIP5 models that have horizontal resolution closer to  $2^\circ$ . de Boer *et al* (2012) analyzed CCSM4 temperatures for the Arctic region just north of our study region and concluded that model temperatures for the present climate were in good agreement with the 40 year European Centre for Medium-Range Weather Forecasts (ECMWF) Re-Analysis (ERA-40). Since CCSM4 annual mean temperatures are somewhat too warm in the more central part of our region (Gent *et al* 2011) and another study found the strength of the CCSM4 snow albedo feedback to be somewhat too low in boreal forests (Thackeray *et al* 2014), we will compare our results for future trends with several of the other CMIP5 models to investigate how robust our results are. We have used the high emission Representation Concentration Pathway 8.5 (RCP8.5) scenario to ensure that trends, if they are present, are most likely to be identified.

Our focus is on how surface air temperatures will change during the 21st century within the region bounded by  $50^\circ$  N– $60^\circ$  N and  $80^\circ$  E– $140^\circ$  E and  $60^\circ$  N– $70^\circ$  N and  $80^\circ$  E– $180^\circ$  E. Our analysis includes only the land grid cells in the climate model output. Figure 1 shows the location of the region in eastern Siberia along with elevation. Model grid cells range in elevation from sea level to 2374 m. As figure 1 shows, the highest elevations are in the south, but there are also high-elevation regions elsewhere in the study region. We examine projected temperature changes within this region for the end of the 21st century by subtracting the average temperature of a six-member model ensemble extracted from the online archive for



the current climate (2006–2025) from the end of century (2081–2100) projections, consistent with the use of these same 20 year averages in IPCC (2014). Of particular interest is how the warming rates vary with both latitude and elevation as well as between summer (JJA) and winter (DJF).

### 3. Latitudinal variability of projected temperature changes

In this section, we focus on the role of Arctic amplification by examining how temperature changes with latitude in both summer and winter. Figures 2(a), (b) show a three-dimensional view of the CCSM4 projected temperature changes for the 21st century during both winter and summer. The view is looking southeastward, and the highest elevation regions can be seen in the southwest, although there are also smaller mountains at the northernmost latitudes. In winter, the warming rates clearly increase from south to north although not uniformly across latitude bands. The winter warming rates are also considerably higher than in summer, and there does not appear to be a significant latitudinal dependence on warming rates in summer. The two figures indicate that some of the smaller rates of warming tend to occur at the higher elevations. We next quantify the variability in the temperature changes with latitude, and in the following section we quantify the variability in the temperature changes with elevation.

Figure 3(a) shows the CCSM4 projected 21st century warming rates as a function of latitude for winter and summer. There is a statistically significant positive latitudinal gradient of  $0.16\text{ }^{\circ}\text{C degree}^{-1}$  of latitude in winter as shown in figure 3(a), which amounts to an increase of about  $3\text{ }^{\circ}\text{C}$  in warming rates from the southern to northern borders of our region. Although

there is a positive gradient in summer, it is much smaller with a rate of about  $0.02\text{ }^{\circ}\text{C degree}^{-1}$  latitude. This is consistent with Arctic amplification, because it indicates that the strongest north/south gradients of warming rates occur in winter when Arctic amplification is most pronounced.

To investigate whether these results are model dependent, we performed the same analysis using averaged ensembles from four other global climate models, and the results are shown in table 1. In winter, all of the models show strong and statistically significant increases in the rates of warming moving northward, although the specific rates vary between  $0.11\text{ }^{\circ}\text{C degree}^{-1}$  and  $0.30\text{ }^{\circ}\text{C degree}^{-1}$  of latitude among the models. In summer, the latitudinal trends are much smaller with both positive and negative values ranging from  $-0.08\text{ }^{\circ}\text{C degree}^{-1}$  to  $+0.02\text{ }^{\circ}\text{C degree}^{-1}$  of latitude. Four of the summer latitudinal trends are statistically significant. As table 1 indicates, the winter results are robust among all of the models, with statistically significant increasing warming rates moving poleward, while in summer, the latitudinal changes are much smaller.

### 4. Elevation-dependent temperature changes

Next, we focus on how elevation affects future warming rates within the region. To investigate whether any elevation dependence might be overwhelmed by the strong influence of Arctic amplification as noted by the large latitudinal temperature gradients shown in figures 2 and 3(a), we examine the dependence of the temperature changes for  $5^{\circ}$  zonally averaged bands across the entire region.

Table 2 shows the magnitude of the warming rates for each  $5^{\circ}$  latitude band as a function of elevation

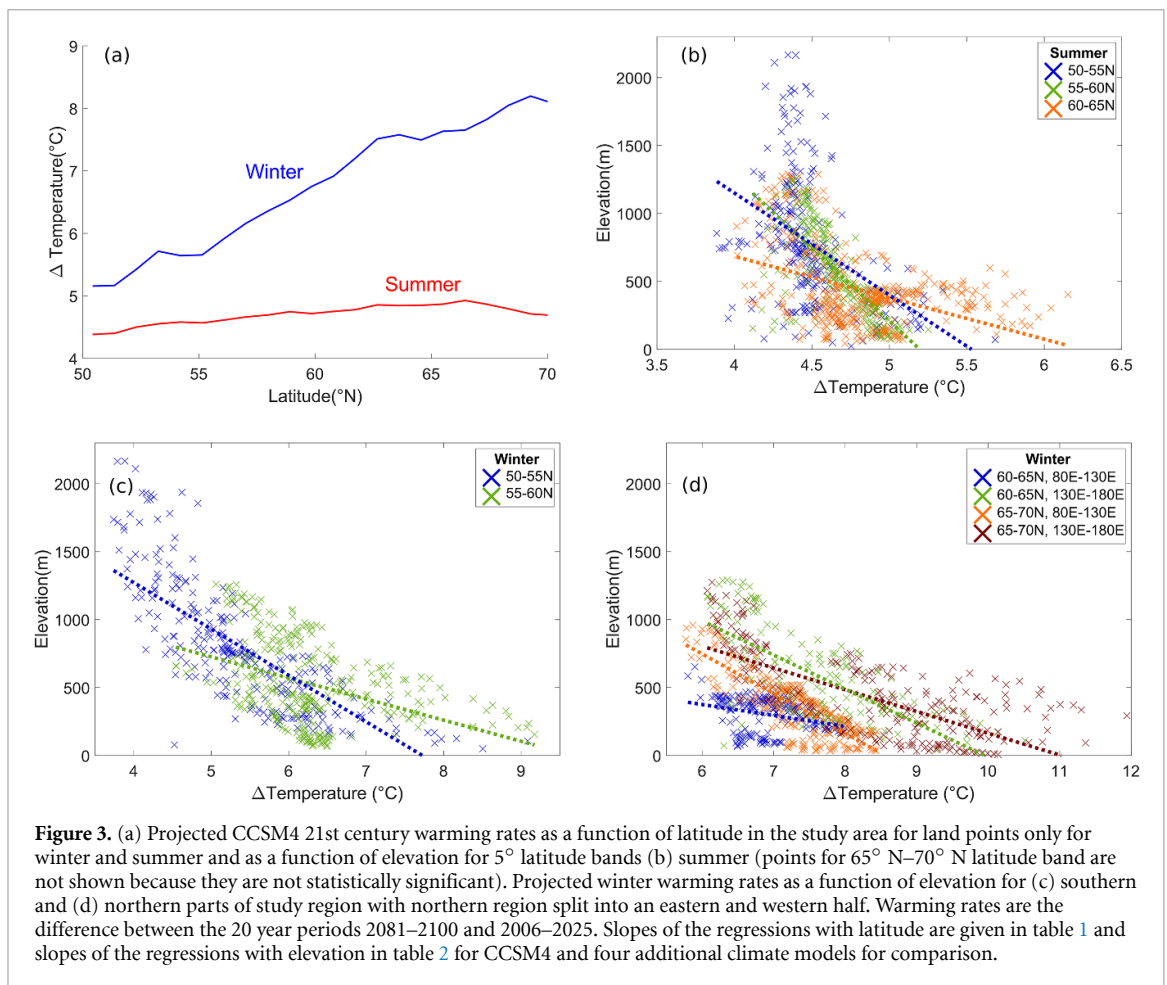
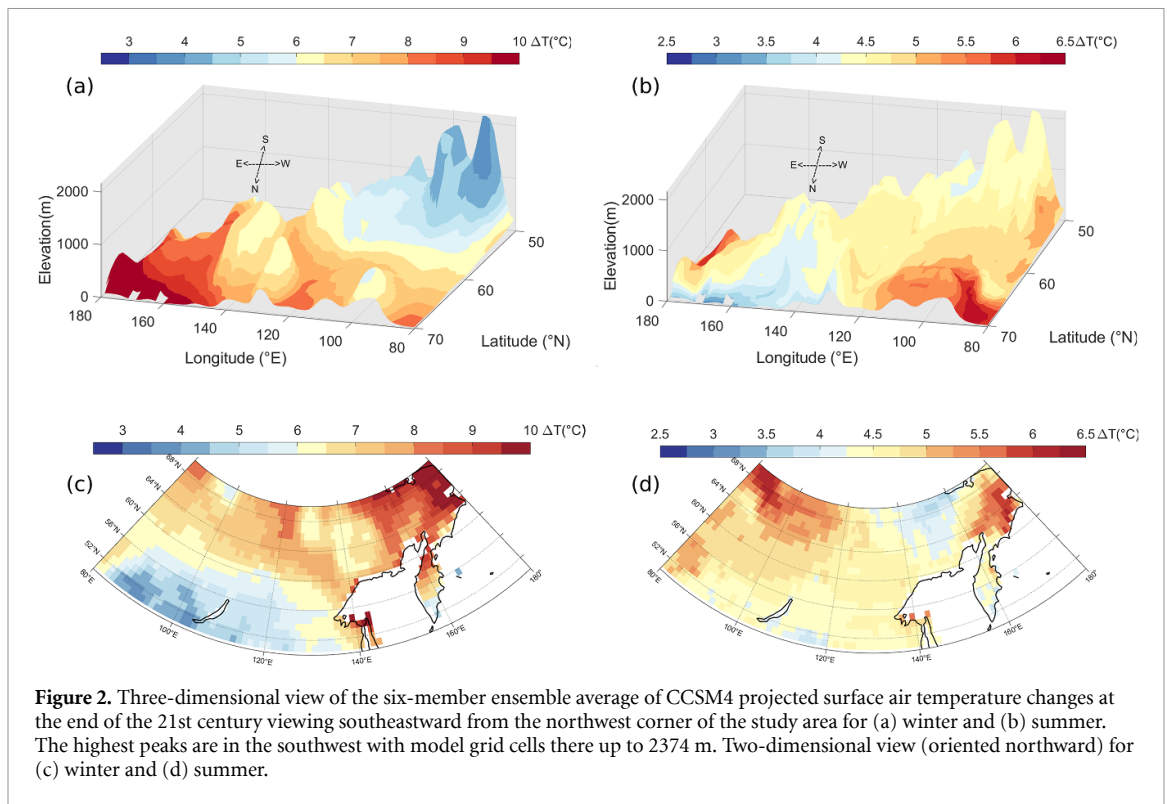


**Table 1.** Changes in future warming rates as a function of latitude ( $^{\circ}\text{C degree}^{-1}$  latitude) for summer and winter within the latitude band  $50^{\circ}\text{N}$ – $70^{\circ}\text{N}$  for the ensemble averages of five climate models in the CMIP5. These models and their latitude–longitude resolutions are the NCAR Community Climate System Model (CCSM4,  $0.9^{\circ}$  by  $1.25^{\circ}$ ), Centre National de Recherches Météorologiques (CNRM-CM5,  $1.4^{\circ}$  by  $1.4^{\circ}$ ), Commonwealth Scientific and Industrial Research Organization (CSIRO-MK360,  $1.85^{\circ}$  by  $1.85^{\circ}$ ), Met Office Hadley Centre (HADGEM2-CC,  $1.25^{\circ}$  by  $1.85^{\circ}$ ) and Max Planck Institute for Meteorology (MPI,  $1.85^{\circ}$  by  $1.85^{\circ}$ ). Regressions that are significant at the 95% level are shown in bold. The number of members in the ensemble average is shown in parenthesis after the model name.

	Slope ( $^{\circ}\text{C degree}^{-1}$ latitude)					Mean
	CCSM4 (6)	CNRM-CM5 (4)	CSIRO-MK360 (6)	HADGEM2-CC (3)	MPI (3)	
Winter	<b>0.16</b>	<b>0.30</b>	<b>0.11</b>	<b>0.30</b>	<b>0.16</b>	<b>0.21</b>
Summer	<b>0.02</b>	<b>−0.04</b>	−0.02	<b>−0.08</b>	<b>0.02</b>	<b>−0.02</b>

**Table 2.** Future warming rate in winter and summer as a function of elevation for the  $5^{\circ}$ -latitude bands spanning  $50^{\circ}\text{N}$ – $70^{\circ}\text{N}$  (with regressions that are significant at the 95% level shown in bold) for five climate models in the CMIP5.

Slopes ( $^{\circ}\text{C km}^{-1}$ )	CCSM4	CNRM-CM5	CSIRO-MK360	HADGEM2-CC	MPI	Mean (Std)	Mean (Std) (without CNRM)
Winter							
$50^{\circ}\text{N}$ – $55^{\circ}\text{N}$	<b>−1.74</b>	<b>−1.75</b>	<b>−0.36</b>	<b>−2.20</b>	<b>−0.53</b>	−1.32 (0.73)	−1.21 (0.78)
$55^{\circ}\text{N}$ – $60^{\circ}\text{N}$	<b>−0.93</b>	0.42	<b>−3.23</b>	<b>−0.84</b>	<b>−0.36</b>	−0.99 (1.22)	−1.34 (1.11)
$60^{\circ}\text{N}$ – $65^{\circ}\text{N}$	<b>−0.70</b>	0.30	<b>−3.33</b>	−0.23	<b>−1.11</b>	−1.01 (1.25)	−1.34 (1.19)
$65^{\circ}\text{N}$ – $70^{\circ}\text{N}$	<b>−2.46</b>	<b>−2.11</b>	<b>−1.97</b>	<b>−3.30</b>	<b>−2.09</b>	−2.39 (0.49)	−2.46 (0.52)
Summer							
$50^{\circ}\text{N}$ – $55^{\circ}\text{N}$	<b>−0.24</b>	0.07	<b>0.47</b>	<b>−0.51</b>	<b>0.25</b>	0.01 (0.35)	−0.01 (0.39)
$55^{\circ}\text{N}$ – $60^{\circ}\text{N}$	<b>−0.48</b>	<b>−0.67</b>	<b>−1.49</b>	<b>−1.91</b>	<b>−0.69</b>	−1.05 (0.55)	−1.14 (0.58)
$60^{\circ}\text{N}$ – $65^{\circ}\text{N}$	<b>−0.56</b>	−0.14	<b>−0.78</b>	<b>−1.14</b>	0.05	−0.51 (0.43)	−0.61 (0.43)
$65^{\circ}\text{N}$ – $70^{\circ}\text{N}$	−0.10	−0.14	−0.22	<b>−0.27</b>	0.04	−0.14 (0.11)	−0.14 (0.12)

( $^{\circ}\text{C km}^{-1}$ ) with numbers in bold being statistically significant at the 5% level. The table shows that all of these values are statistically significant except the highest latitude band in summer. However, although there is EDW, temperatures are increasing at slower rates at higher elevations than they are at their surrounding lower elevation counterparts. This result is in contrast to the majority of studies for mid latitudes that generally show faster warming rates at higher elevations (e.g. Rangwala and Miller 2012, Pepin *et al* 2015).

For winter, the elevation dependence of the CCSM4 projected warming rates is presented in figure 3(b). These rates are statistically significant at all latitudes with negative values ranging between  $−0.70^{\circ}\text{C km}^{-1}$  and  $−2.46^{\circ}\text{C km}^{-1}$  between  $50^{\circ}\text{N}$  and  $70^{\circ}\text{N}$  (table 2). The linear regression lines are shown; we did not investigate whether a non-linear fit to the points would be better since the main point is related to the sign of the relationship. Additionally, elevation and latitude are likely not the only factors affecting the data, as it has been observed that most of the greater and more scattered changes in temperature presented in figure 3(b) in the  $60^{\circ}\text{N}$ – $65^{\circ}\text{N}$  and  $65^{\circ}\text{N}$ – $70^{\circ}\text{N}$  latitude bands are from the Kamchatka Peninsula and its surrounding area, which may be a result of its particularly close proximity to both the Pacific and Arctic oceans. The relationship between temperature change and elevation is statistically significant though, with the elevation dependence appearing strongest for the

southern and northern bands and weaker in the central latitude bands. For summer, the elevation dependence is statistically significant at all but the most northern latitude band and negative at all latitudes with values from  $−0.10^{\circ}\text{C km}^{-1}$  to  $−0.56^{\circ}\text{C km}^{-1}$ . Overall, our results for the  $50^{\circ}\text{N}$ – $70^{\circ}\text{N}$  latitude band indicate that where EDW occurs, it is negative in both summer and winter, with much higher and more statistically significant values in winter than in summer.

As in the previous section, we again investigate how these results compare with the other four global climate models. The winter results are quite robust, with less warming at higher elevations for 18 of the 20 values (5 models and 4 latitude bands) and 17 of the 18 values are statistically significant. Only one model, the CNRM-CM5 model for the  $55^{\circ}\text{N}$ – $60^{\circ}\text{N}$  and  $60^{\circ}\text{N}$ – $65^{\circ}\text{N}$  latitude bands, obtained positive warming with elevation, but neither of those were statistically significant.

As in the previous section, the results are more mixed in summer. There are still negative trends of warming rates with elevation for 15 of the 20 values, but only 11 of them are statistically significant. The summer rates are also much smaller than the winter values at all latitudes for CCSM4, but this picture is more mixed for the other models. Overall the winter results are much more robust than in summer, with much lower rates of future warming at higher elevations than in the lower surrounding regions.

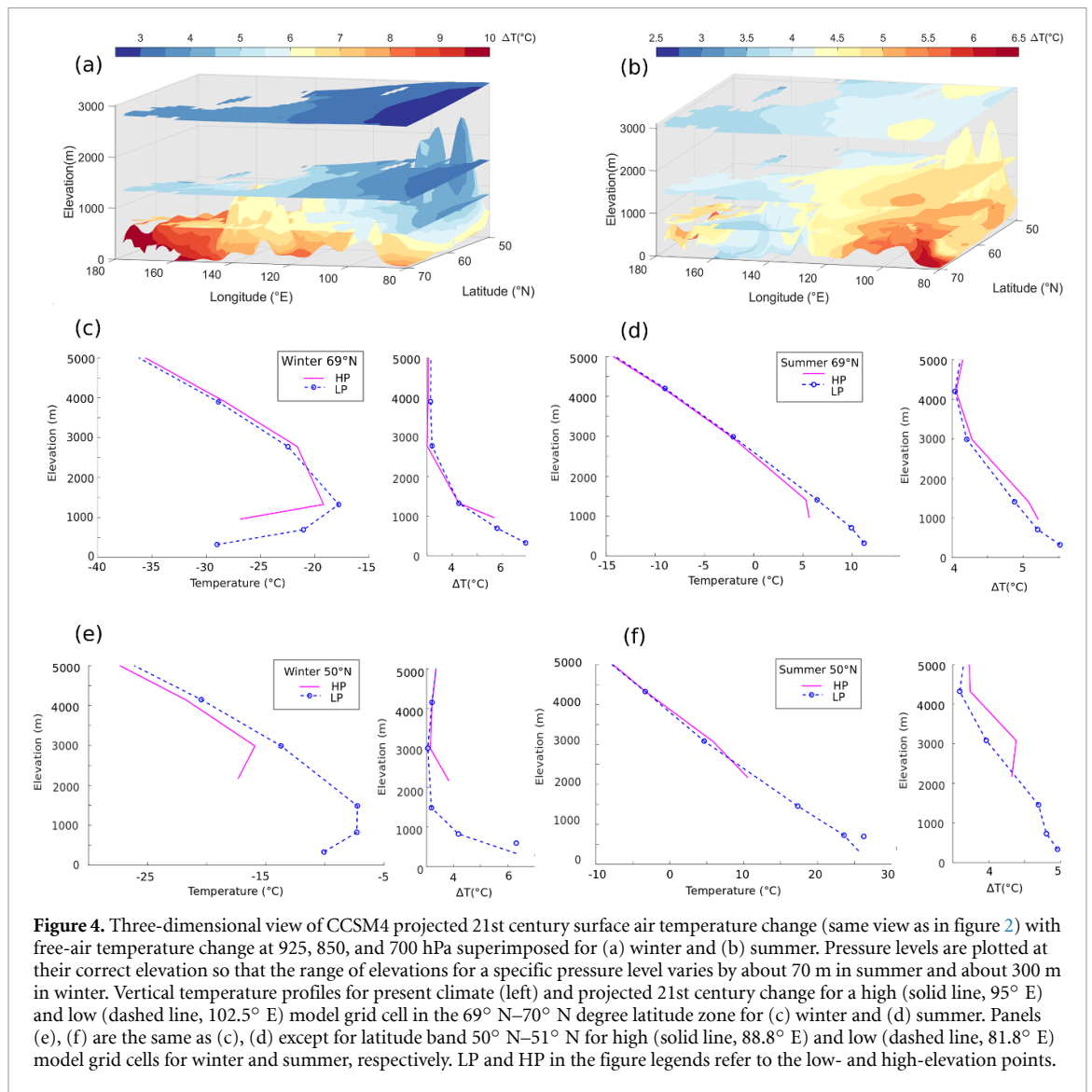


**Figure 4.** Three-dimensional view of CCSM4 projected 21st century surface air temperature change (same view as in figure 2) with free-air temperature change at 925, 850, and 700 hPa superimposed for (a) winter and (b) summer. Pressure levels are plotted at their correct elevation so that the range of elevations for a specific pressure level varies by about 70 m in summer and about 300 m in winter. Vertical temperature profiles for present climate (left) and projected 21st century change for a high (solid line, 95° E) and low (dashed line, 102.5° E) model grid cell in the 69° N–70° N degree latitude zone for (c) winter and (d) summer. Panels (e), (f) are the same as (c), (d) except for latitude band 50° N–51° N for high (solid line, 88.8° E) and low (dashed line, 81.8° E) model grid cells for winter and summer, respectively. LP and HP in the figure legends refer to the low- and high-elevation points.

## 5. Free-air temperatures and lapse rate changes

Many different mechanisms have been mentioned as reasons for EDW in other regions including the effects of changes in snow/albedo, water vapor, free-air temperatures, and Planck black body radiation (Ohmura 2012, Rangwala and Miller 2012, Pepin *et al* 2015). In this section, we focus primarily on changes in free-air temperatures, winter inversions, and vertical lapse rates. We briefly discuss the other mechanisms in the next section.

Figures 4(a) and (b) show the same three-dimensional view of the projected 21st century changes in surface air temperatures as in figures 2(a), (b), but with projected temperature changes at three additional elevations (925 hPa, 850 hPa, 700 hPa) superimposed. Figure 4(a) shows that, in winter, the free-air temperatures are projected to increase during the 21st century but that the upper level temperatures are generally increasing less than many of the surface temperatures. In addition, it is clear from

figure 4(a) that there is much greater variability in surface air temperature trends than free-air temperatures throughout the region. Although there is some variability in the free-air temperatures, they appear to be only modestly affected by the presence of peaks that reach up to those levels with free-air temperature trends tending to be somewhat larger near those peaks.

To quantify the above, we calculate the mean temperature trends and standard deviations of the trends over the entire study area for each of the elevations shown in figure 4. In winter, the mean 21st century change in surface air temperature is 6.7 °C and decreases upward to 3.3 °C at 700 hPa; similarly, the standard deviation decreases upward from 1.8 °C to 0.4 °C. In summer, the mean surface temperature increases are smaller (4.7 °C) than in winter and decrease upward to 4.0 °C at 700 hPa, but the standard deviations decrease upward from 0.66 °C at the surface to 0.34 °C at 700 hPa. Figure 4(b) shows that there is a much smaller range of temperature change in summer than in winter for both the surface air

temperature as well as the free-air temperature. One interesting difference is that the free-air temperature trends at 850 hPa decrease toward the continental interior (toward southwest) in winter but increase toward the continental interior in summer.

To investigate this effect further, we next examine for winter and summer two sets of changes in vertical temperature profiles, one set for a high- and low-elevation site for a lower latitude and another set for a higher latitude (figures 4(c)–(f)). Figure 4(c) shows winter temperature profiles at the beginning of the 21st century and how they are projected to change at the end of the century as a function of elevation for the highest elevation model grid cell and for one of the lowest elevations in the latitude band between 65 and 70° N. For the low-elevation site, there is a very strong temperature inversion that tends to stabilize the atmosphere. This leads to much greater changes in surface temperature (about 8 °C) than in temperatures at 925 hPa (~5.5 °C). For the high-elevation site, the surface is at 890 hPa, and the change in temperature there is the same as the temperature change at the low-elevation site at the same latitude at that level. Figures 4(e) and (f) shows the same changes as in figures 4(c) and (d) but for high- and low-elevation grid cells in a latitude band on the southern side of our study region (50° N–55° N). The winter results are similar to the higher latitude band, although the absolute temperature changes are smaller. The air temperatures warm more at the surface than in the layers above at the low-elevation site, and the temperature changes at 850 hPa are within a degree of each other for both sites, again indicating that the changes in surface temperature at the high-elevation sites are strongly connected to changes in free-air temperatures.

The 50° N–55° N band is a bit different from the other latitude bands because some of the largest temperature changes with elevation in winter occur in that band. However, the inversion in this band (see figure 4(e)) is much smaller than for the highest latitude band. This band is in the transition region between the lower latitudes where we have previously found enhanced projected warming at higher elevations in the Tibetan Plateau (Rangwala *et al* 2010) and the higher latitudes in this paper where the reverse is occurring. Other processes, such as snow albedo, are involved here. In particular, we find that in the southwest corner of the 50° N–55° N band the snow cover decreases the most at the lowest elevations (not shown) where temperatures (see figure 2(a)) are increasing the most.

Figure 4(d) shows that the temperature changes in summer in the highest latitude band are smaller than in winter at both the high- and low-elevation sites. Figure 4(f) shows the same result for the lowest latitude band. There is very little variation with height at the low-elevation site. However, consistent with the winter case, free-air temperature increases

less than surface temperature throughout the study region. However, as previously noted in this section, the area-wide averaged summertime surface temperature increases are only 0.7 °C greater than at 700 hPa as compared to 3.4 °C greater in winter. This explains much of our significantly more robust result that future projected winter warming rates will be smaller at higher elevations but generally similar to or somewhat smaller in summer at high latitudes.

## 6. Summary and conclusions

The focus of this paper is on the effects of elevation and Arctic amplification on projected climate change in eastern Siberia. The future projections are based on the differences between two 20 year periods (2081–2100 minus 2006–2025) of climate model simulations from the CCSM4 and four other RCP8.5 experiments in the CMIP5 archives. The projected temperature changes are strongly dependent on latitude, with annual warming rates increasing northward by 0.16 °C degree<sup>-1</sup> of latitude in winter and 0.02 °C degree<sup>-1</sup> of latitude in summer for the CCSM4. These latitudinal gradients are much stronger in winter, as one might expect, because Arctic amplification is much stronger in winter than in summer.

A study by Wang *et al* (2016) used a set of global observations to examine the relative roles of Arctic amplification and elevation on warming rates during the 1961–2010 period. They found that globally higher elevation regions have been warming at faster rates than lower elevations. They also found that temperatures were increasing faster at higher latitudes. Unlike their observational study, which was global, our analysis of future projections from climate models are for north of 50° N in eastern Russia, a region for which Wang *et al* (2016) had relatively few observations.

To investigate the role of elevation in future climate change in this region, we first removed the latitudinal influence of Arctic amplification by examining the land mass in 5° latitude bands between 50° N and 70° N. Within these latitude zones, we do find EDW in the CCSM4 simulation; however, unlike most mid-latitude locations where warming rates are greater at higher elevations, we find that future warming rates are smaller at higher elevations in this high-latitude region with values ranging between -0.70 °C km<sup>-1</sup> and -2.46 °C km<sup>-1</sup> in winter, when the elevation-dependent gradients are largest. This elevation dependence is statistically significant at all latitudes. The summer season is more complex, with elevational warming gradients ranging between -0.10 °C km<sup>-1</sup> to -0.56 °C km<sup>-1</sup> and statistically significant at most latitudes. We found that the EDW results are generally consistent with those based on four other climate model simulations from the CMIP5 archives.

We have shown that much of the elevation dependence on warming rates can be attributed to changes in free-air temperatures, particularly in winter. At the highest latitudes, there are very strong temperature inversions in winter, and these strong inversions prevent the strong Arctic amplification of surface air temperature to penetrate too high into the atmosphere. This means that free-air temperatures are projected to warm less than surface temperatures throughout much of our region, but these differences are most pronounced at the highest latitudes. As a result, temperature changes in mountains that penetrate higher into the atmosphere are responding primarily to changes in free-air temperatures at those levels.

These results are consistent with other studies that have shown very strong inversions in the northern part of our study region. Both Serreze *et al* (1992) and Zhang *et al* (2011) found the frequency of inversions, the inversion depth, and the temperature difference across the inversion layer increase from the Norwegian Sea eastward toward the Laptev and East Siberian seas, most likely because of the proximity to the Arctic Ocean. In fact, there is evidence that the Arctic wintertime temperature inversion provides a positive feedback by enhancing Arctic amplification, which is primarily manifested at the surface (Bintanja 2011). Although the qualitative nature of our results appears to be quite robust, namely greater projected warming near the surface than at the top of the planetary boundary layer, the exact magnitude of these differences requires further research. Medeiros *et al* (2011) did a multi-model study and found that models often overestimated the strength of the inversion but they did find that low-level inversions are a stable primary mode over the interior Arctic Ocean and adjacent continents. Similarly, Pavelsky *et al* (2011) found that although global climate models do obtain Arctic inversions, they often do less well in characterizing the strength of the inversions.

Among the other processes that have been attributed to causing EDW, changes in snow cover and surface albedo have some impact on our results but more so in transition seasons because changes in snow cover are not that large in our study. Considering that snow cover was small at the beginning of summer, any decreases were also small. Snow cover was initially high in winter and stayed relatively high. In the highest elevation region in the southwestern portion of our study region, the snow albedo effect does appear to account for some of the elevation-dependent trends there as more snow melts at the lower elevations, which is consistent with greater warming at lower elevations there. The Planck black body mechanism probably does contribute somewhat to the north–south gradients of warming rates in winter because the argument is based on the assumption that for a given change in longwave radiation, the temperature change attributed to it will be greater at lower temperatures. However, this

goes in the wrong direction for explaining the negative change in warming rates with elevation. We found that water vapor does increase in the future but tends to increase less at higher latitudes in winter. However, since the sensitivity of downward longwave radiation to increases in water vapor is greater at higher latitudes where the atmosphere is drier, the changes in water vapor do affect the future temperature changes.

Our overall finding here is that the free-air temperature changes are the primary reason why temperatures are changing more slowly at the higher elevations in this high-latitude region, particularly in winter. Arctic amplification itself is dependent on multiple feedbacks, including the snow/ice albedo and water vapor feedbacks, but the primary reason for the elevation-dependent cooling in winter is that the strong temperature inversion keeps the impact of these feedbacks near the surface so that future temperature changes are greater at the surface than at higher levels. This result is consistent with Bintanja *et al* (2011) who found that the strong Arctic wintertime surface inversion increases Arctic amplification because it confines the surface warming to close to the surface so that this warming contributes little to outgoing infrared radiation.

Understanding climate change in high northern latitudes is important because one key dynamic process in the region is the relationship between decreasing Arctic sea ice and its impact on weather and climate over the nearby land mass. In fact, Ghatak *et al* (2012) and Cohen *et al* (2013) found that loss of Arctic sea ice may result in Siberian snow; Francis and Vavrus (2012, 2015) suggest that loss of sea ice may affect mid-latitude regions. Research efforts to understand these dynamics should be prioritized given the rapid and widespread changes in sea ice and their potentially large impacts on regional climate.

## Data availability statement

The data that support the findings of this study are available upon reasonable request from the authors.

## Acknowledgments

JEF and JMF acknowledge support from the Rutgers University Aresty Center Research Program. This project received support from the New Jersey Agricultural Experiment Station and the USDA-National Institute for Food and Agriculture, Hatch Project Number NJ32116. MJP gratefully acknowledges support from the United Nations Development Programme and the NASA-Columbia cooperative agreement ‘Interdisciplinary Research on Earth System Modeling and the Impacts of Climate Change’ (Federal Award ID Number 80NSSC17M0057).

## ORCID iDs

James R Miller  <https://orcid.org/0000-0002-6376-7976>

Michael J Puma  <https://orcid.org/0000-0002-4255-8454>

Joseph M Finnegan  <https://orcid.org/0000-0001-7925-4289>

## References

- Beniston M, Diaz H F and Bradley R S 1997 Climatic change at high elevation sites: an overview *Clim. Change* **36** 233–51
- Bintanja R, Graverson R G and Hazeleger W 2011 Arctic winter warming amplified by the thermal inversion and consequent low infrared cooling to space *Nat. Geosci.* **4** 758–61
- Bradley R S, Keimig F T and Diaz H F 2004 Projected temperature changes along the American cordillera and the planned GCOS network *Geophys. Res. Lett.* **31** 16
- Cohen J, Jones J, Furtado J C and Tziperman E 2013 Warm Arctic, cold continents: a common pattern related to Arctic sea ice melt, snow advance, and extreme winter weather *Oceanography* **26** 150–60
- de Boer G, Chapman W, Kay J E, Medeiros B, Shupe M D, Vavrus S and Walsh J 2012 A characterization of the present-day Arctic atmosphere in CCSM4 *J. Clim.* **25** 2676–95
- Diaz H F and Bradley R S 1997 Temperature variations during the last century at high elevation sites *Climatic Change at High Elevation Sites* (Berlin: Springer) pp 21–47
- Francis J A and Vavrus S J 2012 Evidence linking Arctic amplification to extreme weather in mid-latitudes *Geophys. Res. Lett.*, **39** L06801
- Francis J A and Vavrus S J 2015 Evidence for a wavier jet stream in response to rapid Arctic warming *Environ. Res. Lett.* **10** 014005
- Fyfe J C and Flato G M 1999 Enhanced climate change and its detection over the Rocky Mountains *J. Clim.* **12** 230–43
- Gelfan A, Gustafsson D, Motovilov Y, Arheimer B, Kalugin A, Krylenko I and Lavrenov A 2017 Climate change impact on the water regime of two great Arctic rivers: modeling and uncertainty issues *Clim. Change* **141** 499–515
- Gent P R *et al* 2011 The community climate system model version 4 *J. Clim.* **24** 4973–91
- Ghatak D, Deser C, Frei A, Gong G, Phillips A, Robinson D A and Stroeve J 2012 Simulated Siberian snow cover response to observed Arctic sea ice loss, 1979–2008 *J. Geophys. Res.* **117** D23
- Ghatak D and Miller J 2013 Implications for Arctic amplification of changes in the strength of the water vapor feedback *J. Geophys. Res.* **118** 7569–78
- IPCC 2014 *Synthesis Report: Contribution of Working Groups I, II and III to the Fifth Assessment Report of the Intergovernmental Panel on Climate Change* (IPCC) ed R K Pachauri and L Meyer (Geneva: Intergovernmental Panel on Climate Change) p 151
- Krysanova V and Hattermann F F 2017 Intercomparison of climate change impacts in 12 large river basins: overview of methods and summary of results *Clim. Change* **141** 363–79
- Manabe S, Milly P C D and Wetherald R 2004 Simulated long-term changes in river discharge and soil moisture due to global warming *Hydrol. Sci. J.* **49** 625–42
- Medeiros B, Deser C, Tomas R A and Kay J E 2011 Arctic inversion strength in climate models *J. Clim.* **24** 4733–40
- Miller J R, Chen Y, Russell G L and Francis J A 2007 Future regime shift in feedbacks during Arctic winter *Geophys. Res. Lett.* **34** L23707
- Miller J R and Russell G L 1992 The impact of global warming on river runoff *J. Geophys. Res.* **97** 2757–64
- Milly P C, Dunne K A and Vecchia A V 2005 Global pattern of trends in streamflow and water availability in a changing climate *Nature* **438** 347–50
- Ohmura A 2012 Enhanced temperature variability in high-altitude climate change *Theor. Appl. Climatol.* **110** 499–508
- Pavelsky T M, Boé J, Hall A and Fetzer E J 2011 Atmospheric inversion strength over polar oceans in winter regulated by sea ice *Clim. Dyn.* **36** 945–55
- Pepin N *et al* 2015 Elevation-dependent warming in mountain regions of the world *Nat. Clim. Change* **5** 424–30
- Rangwala I and Miller J R 2012 Climate change in mountains: a review of elevation-dependent warming and its possible causes *Clim. Change* **114** 527–47
- Rangwala I, Miller J R, Russell G L and Xu M 2010 Using a global climate model to evaluate the influences of water vapor, snow cover and atmospheric aerosol on warming in the Tibetan Plateau during the twenty-first century *Clim. Dyn.* **34** 859–72
- Rawlins M A *et al* 2010 Analysis of the Arctic system for freshwater cycle intensification: observations and expectations *J. Clim.* **23** 5715–37
- Scherrer S C, Ceppi P, Croci-Maspoli M and Appenzeller C 2012 Snow-albedo feedback and Swiss spring temperature trends *Theor. Appl. Climatol.* **110** 509–16
- Screen J A and Simmonds I 2010 The central role of diminishing sea ice in recent Arctic temperature amplification *Nature* **464** 1334–7
- Serreze M C, Barrett A P, Stroeve J C, Kindig D N and Holland M M 2009 The emergence of surface-based Arctic amplification *Cryosphere* **3** 11–19
- Serreze M C and Francis J A 2006 The Arctic amplification debate *Clim. Change* **76** 241–64
- Serreze M C, Schnell R C and Kahl J D 1992 Low-level temperature inversions of the Eurasian Arctic and comparisons with Soviet drifting station data *J. Clim.* **5** 615–29
- Sévellec F, Fedorov A V and Liu W 2017 Arctic sea-ice decline weakens the Atlantic meridional overturning circulation *Nat. Clim. Change* **7** 604–10
- Sharma A R and Déry S J 2016 Elevational dependence of air temperature variability and trends in British Columbia's Cariboo Mountains, 1950–2010 *Atmos.-Ocean* **54** 153–70
- Solomon S, Qin D, Manning M, Chen Z, Marquis M, Averyt K B, Tignor M and Miller H L 2007 *Climate Change 2007: The Physical Science Basis* (Cambridge: Intergovernmental Panel on Climate Change, Cambridge University Press)
- Symon C, Arris L and Heal B (ed) 2005 *Arctic Climate Impact Assessment: ACIA* (Cambridge: Cambridge University Press)
- Thackeray C W, Fletcher C G and Derksen C 2014 The influence of canopy snow parameterizations on snow albedo feedback in boreal forest regions *J. Geophys. Res.* **119** 9810–21
- Wang Q, Fan X and Wang M 2016 Evidence of high-elevation amplification versus Arctic amplification *Sci. Rep.* **6** 1–8
- Zhang Y, Seidel D J, Golaz J C, Deser C and Tomas R A 2011 Climatological characteristics of Arctic and Antarctic surface-based inversions *J. Clim.* **24** 5167–86